The effect of thallium addition on differential thermal analysis of glassy selenium. Part 1

M. F. KOTKATA
Physics Department, Faculty of Science, Ain Shams University, Cairo, Egypt

M. H. EL-FOULY, S. A. FAYEK
National Centre for Radiation Research and Technology, Cairo, Egypt

The effect of thallium on the phenomena accompanying the thermally induced structural changes in different compositions of the chalcogenide system Tl_xSe_{1-x}, with $x = 0.0$ to 0.9, has been investigated using differential thermal analysis measurements. It is possible to prepare massive homogeneous glassy samples with thallium contents up to 10 at%. Glasses with some embedded crystallites are obtained up to 40 at% Tl. The coefficient of the glass-forming tendency (K_{gl}) increases with increasing selenium content. In the binary system Tl–Se, one (or more) of the phases are likely to be more unstable with respect to crystallization than was the initially homogeneous system. The activation energy of crystallization for the glasses from $x = 0.0$ to 0.3, varies from 1.0 to 4.5 eV for the low-temperature phase and from 1.7 to 2.5 eV for the high-temperature phase.

1. Introduction

The concept of "reaction temperature", when the heat produced in a solid-state reaction causes an appreciable temperature rise, was used in early studies and is related to the kinetics of the reaction. This method has evolved into the technique of differential thermal analysis (DTA) which has developed rapidly in recent years. It is undoubtedly of great value as a qualitative tool for the study of solid state reactions. Different reactions in DTA and the thermal properties of the sample indicate a deflection from the base line, or peaks. That is, the scanning character of DTA provides a thermal spectrum of the characteristic transitions, such as glass transition (at temperature T_g), crystallization exotherm (with maximum crystallization rate occurring at temperature T_c), and melting endotherm (with melting point T_m).

Crystallization during heating or cooling results in an exothermic peak (or peaks) and melting of crystalline material yields an endothermic peak (or peaks). However, if the reaction occurs at different heating rates, the position (start–peak–end) of the exothermic peak varies. It was demonstrated that this variation in exothermic peak temperature could be used to determine the activation energy of crystallization [1, 2].

In a previous paper [3], X-ray diffraction has been used to study the effect of the addition of thallium on the structural variations of amorphous as well as recrystallized selenium. Also, a short review about the thermal character of the binary system Tl–Se has been published [4].

In this paper, a detailed investigation is made of the phenomena accompanying the thermally induced structural changes in various compositions of the system Tl_xSe_{1-x} using numerous DTA thermograms. The effect of thallium on the crystallization kinetic parameters of glassy selenium is also studied.

2. Experimental details

A series of massive alloys having the general formula Tl_xSe_{1-x}, with $x = 0.0$ to 0.9, were prepared for the present investigation. The necessary quantities from the elements selenium and thallium (purity 99.999%) required for the preparation of 10 g of each composition were weighed using an electrical balance with an accuracy of 10^{-4} g. The weighed materials were loaded into dry, clean, quartz ampoules (~ 16 mm diameter) sealed under a vacuum of 10^{-5} mm Hg. Synthesis of the samples was carried out in the following temperature steps: heating the ampoules up to 400° C and holding at this temperature for 2 h, and then the furnace temperature was raised to 600° C and synthesis was continued for another 4 h during which the molten materials were occasionally shaken vigorously to ensure homogeneous mixing of the samples. The melts were then rapidly quenched in ice–water with the ampoules in a horizontal position. This method of preparation leads to the preparation of some of the compositions in the glassy phase.

To obtain the DTA thermograms, 25 mg powder of the freshly quenched (as-prepared) material was put in an aluminium sample pan. The latter was immediately introduced in its place in the DTA apparatus (Shimadzu model DT-30) and a constant heating rate was applied. The differences ΔT, between the sample temperature and that of the reference (α-Al_2O_3) were recorded directly as a function of the furnace temperature (T) using a double-pen recorder. Heating rates of 2, 5, 10, 20, 30 and 50° C min^{-1} were used.
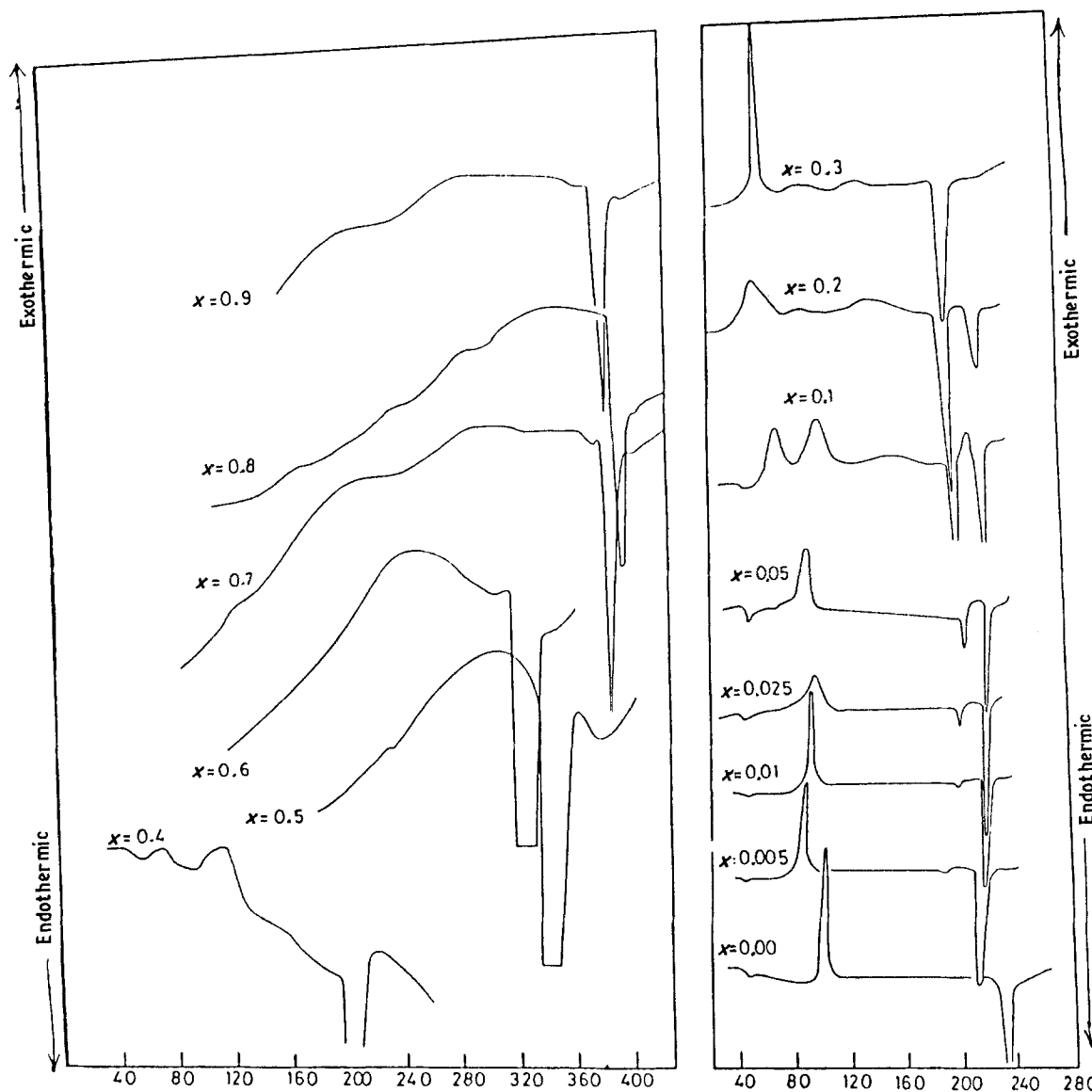
Figure 1 DTA thermograms for $Tl_x Se_{1-x}$ as-prepared (ice–water quenching from melts) samples scanned at a heating rate of $10°C\,min^{-1}$.

3. Effect of composition on thermal transition

Fig. 1 shows typical DTA traces of freshly prepared $Tl_x Se_{1-x}$ samples taken at a constant heating rate of $10°C\,min^{-1}$ (as an example). In this figure, the endotherms due to the glass transition occurred at temperatures ranging from 40 to 47°C depending on thallium content in the glassy range from $x = 0.0$ to 0.1. Such an appearance of T_g, for $x = 0.0$ to 0.1, confirms the X-ray results that show no characteristic peaks for Tl–Se compositions having thallium contents up to 10 at % [3]. For compositions $x = 0.2, 0.3$ and 0.4 no glass transition temperature appears in spite of the presence of an exothermic peak (or peaks) on the DTA traces. This may be due to the presence of a considerable amount of minute crystal sites as indicated by a few weak diffraction lines in their X-ray spectrum [3].

Following the glass transition, the exotherm due to the crystallization of samples at $10°C\,min^{-1}$ yields one or two exothermic peaks depending on thallium content. The materials in the composition region from $x = 0.0$ to 0.025 give one crystallization peak lying in the temperature range 86 to 103°C depending on thallium content in a non-regular manner as is shown

in Table I. The compositions having a thallium content in the region $x = 0.05$ to 0.4 show two crystallization peaks; the first lies in the range 63 to 75°C and the second in the range 88 to 110°C.

Melting of the crystalline materials also yields one or two endothermic peaks depending on thallium content. For compositions $x = 0.0$ and 0.3, there is one melting peak at 220 and 198°C, respectively. For other compositions up to $x = 0.4$, the first T_m lies in the range 190 to 200°C and the second T_m lies in the range 214 to 277°C.

Compositions having a thallium content greater than 40% are crystalline where neither T_g nor T_c were observed, Fig. 1. Two melting points at 331 and 367°C were observed for the composition having equal proportions of thallium and selenium, i.e. $Se_{0.5}Tl_{0.5}$, and for both $Se_{0.3}Tl_{0.7}$, at (364, 375°C) and $Se_{0.2}Tl_{0.8}$ at (380, 395°C). One melting point was observed for the compositions $x = 0.6$ and 0.9 at 312 and 365°C, respectively.

The numerical values of the coefficient of the glass-forming tendency, K_{gl}, have been calculated for the completely glassy materials ($x = 0.0$ to 0.1) according to the formula

$$K_{gl} = (T_c - T_g)/(T_m - T_c)$$

The value of K_{gl} was calculated for the different heating rates ($\phi = 2$ to $50°C\,min^{-1}$) as T_c is greatly heat-rate-dependent, and only the average value of K_{gl} is given in Table I as a function of composition. The results show that the value of K_{gl} almost increases with increasing selenium content. The last result is in agreement with the observation that it is not easy to prepare glasses in bulk form where the thallium content is higher.

4. Effect of heating rate on exothermic peaks

Fig. 2 shows DTA thermograms of amorphous selenium scanned at different rates, ϕ, in the range 2 to $50°C\,min^{-1}$. As ϕ increases, the areas under the crystallization and melting peaks become larger, until $\phi = 30°C\,min^{-1}$ and then decrease for $\phi = 50°C\,min^{-1}$. The peak of the crystallization exotherm increases from 95 to $130°C$ as ϕ increases from 2 to $50°C\,min^{-1}$.

Turnbull [5] has pointed out that the resistance of liquids and glasses to nucleation implies something about their structure. If an amorphous material contained microcrystalline regions, there would be no nuclear barrier, and the crystallization kinetics would be limited by the grain growth. Thus, at temperatures below the melting point, slow crystallization kinetics would indicate that nucleation was required. With respect to glassy selenium, it seems that during slow heating the growth is suppressed by viscosity when the
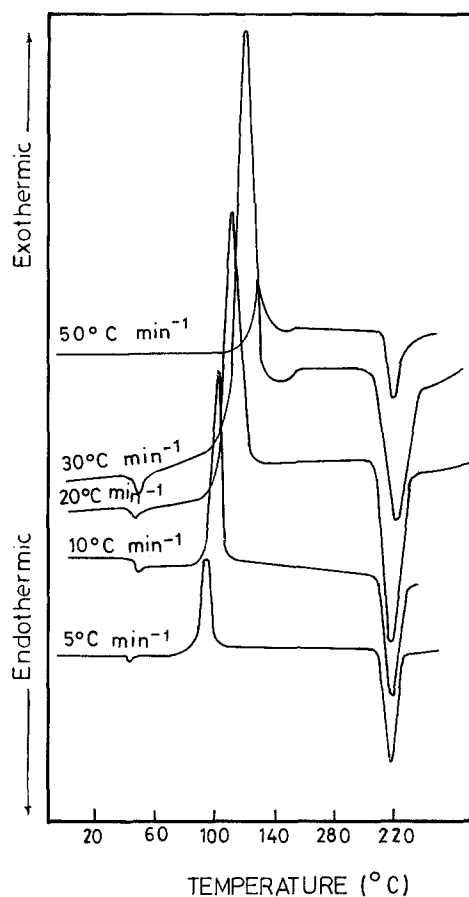
Figure 2 DTA thermograms of glassy selenium samples scanned at different heating rates.

TABLE I DTA data of the investigated compositions in the system Tl_xSe_{1-x}

Composition	$T_g(°C)$	$T_m(°C)$	$2°C\,min^{-1}$			$5°C\,min^{-1}$			$10°C\,min^{-1}$			$20°C\,min^{-1}$			$30°C\,min^{-1}$			$50°C\,min^{-1}$			K_{gl}
			Start	Peak	End	Start	Peak	End	Start	Peak	End	Start	Peak	End	Start	Peak	End	Start	Peak	End	
Se	45	220	80	95	104	85	95	110	90	103	115	80		115	125	84	123	135	105	130	142	0.61
$x = 0.005$	40	190	60	80	92	64	83	114	68	86	105	70	89	110	76	93	120	66	96	138	0.47
		210																			0.38
$x = 0.01$	46	195	48	65	75	52	78	105	60	93	110	64	102	130	80	102	120	90	104	120	0.44
		215																			0.37
$x = 0.025$	44	198	64	80	120	55	87	120	60	93	115	65	100	124	80	105	130	85	111	144	0.45
		215																			0.39
$x = 0.05$	45	200	56	62	72	60	70	76		75												0.15
		219	72	88	100	76	85	120	80	90	110	64	95	126	78	100	120	80	115	140	0.36
$x = 0.1$	47	195	56	65	74	63	71	78	60	72	90	60	72	85	60	75	87	60	80	98	0.15
		220	76	86	104	81	93	100	90	102	120	85	102	124	92	104	124	98	110	124	0.38
$x = 0.2$		193	40	58	76	40	60	78	40	63	78	40	66	78	40	70	82	40	75	100	
		215	66	78	96	78	86	98	78	88	108	78	96	110	92	106	120	100	115	130	
$x = 0.3$		198	50	64	74	44	70	84	60	72	92	60	74	78	50	88	130	60	90	130	
			74	86	100	84	94	120	92	95	102	80	96	120							
$x = 0.4$		199				50	65	81	58	66	81	60	73	95	63	74	93	64	76	96	
		277				90	104	115	93	110	126	95	120	140	93	125	140	96	131	150	
$x = 0.5$		331																			
		367																			
$x = 0.6$		312																			
$x = 0.7$		364																			
		375																			
$x = 0.8$		380																			
		395																			
$x = 0.9$		365																			

condition for crystallization is optimum as is clear from Fig. 2. The last statement is true up to $\phi = 30°\,C\,min^{-1}$ where the area under the exothermic peak becomes larger with increasing ϕ. For $\phi = 50°C\,min^{-1}$, it seems that high growth happens when nucleation is not optimum.

The DTA traces for glass $Se_{0.995}Tl_{0.005}$ show identical behaviour to that of glassy selenium, except the appearance of a trace of a second melting peak started at $190°\,C$ before the original one, and as ϕ increases the areas under the crystallization and melting peaks increase monotonically up to $\phi = 50°C\,min^{-1}$. The addition of 0.5 at % Tl to pure selenium leads to a decrease in the characteristic (start–peak–end) values of crystallization peaks at the different heating rates. The values of the temperature at the exotherm peaks of the composition $x = 0.005$ vary between 80 and $96°\,C$ in the range $\phi = 2$ to $50°C\,min^{-1}$, Table I.

The compositions of $x = 0.01$ and 0.025 show the same behaviour as that of $x = 0.005$ with the exception that area of the second peak which appears after adding thallium increases with the thallium content. For the compositions of $x = 0.05$ and 0.1, a second crystallization peak appears before the original one and the two peaks which appear (crystallization and melting) grow bigger at the expense of the original ones.

Interestingly, when adding more thallium, the original crystallization and melting peaks become smaller so that the new peaks grow bigger than the original ones, as for composition $Se_{0.8}Tl_{0.2}$.

For composition $x = 0.3$, the original peaks nearly disappear and the DTA traces show a large crystallization peak and a trace of another one and a melting peak.

For composition $Se_{0.6}Tl_{0.4}$, it seems that the material at the start is partially crystalline as is clear from the size of the crystallization peaks (two), Fig. 1. It is interesting that, again, two crystallization peaks appear on the traces and two melting peaks appear at high heating rates (30 and $50°C\,min^{-1}$). At low heating rates (5 and $10°C\,min^{-1}$) the size of the first melting peak is smaller than at higher heating rates, while the second melting peak appears at heating rates of 30 and $50°C\,min^{-1}$ only. The disappearance of the second melting peak at low heating rates may be due to a fusion process, as the size of the crystallization peaks is the same at all rates, so the amount of the crystalline phase is the same (of course including the amount of the crystalline phase in the sample before heating). Also, it is found that the size of the melting

peaks increases as the crystallization peaks come closer to the melting peaks, i.e. at high ϕ.

5. DTA cyclic scanning

For compositions of $x = 0.1, 0.3$ and 0.4, $300°\,C$ was chosen as a maximum temperature to be far from the decomposition region (after some preliminary thermogrametry results).

For compositions of $x = 0.5, 0.66, 0.7$ and 0.8, $500°\,C$ was chosen as the maximum temperature to cover most of the probable transition range.

The normal procedure for the DTA cyclic is as follows:

Run a, raise the DTA temperature with heating rate $20°\,C\,min^{-1}$ from room temperature up to 300 or $500°\,C$.

Run b, lower the temperature down to $50°\,C$ at the natural cooling rate of the DTA device, i.e. at an average rate of about $15°\,C\,min^{-1}$.

Run c, raise the temperature again up to 300 or $500°\,C$.

Run d, lower the temperature down to room temperature.

1. For composition $Se_{0.9}Tl_{0.1}$ (Fig. 3a), the DTA traces show a glass transition temperature $T_g = 47°\,C$, two crystallization peaks $(T_{c_1} = 72°\,C, T_{c_2} = 102°\,C)$ and two melting peaks $(T_{m_1} = 195°\,C, T_{m_2} = 220°\,C)$ on Run a. On Run b during cooling, there are two unresolved crystallization peaks $(T_{c_1} = 134°\,C$ and $T_{c_2} = 130°\,C)$. On Run c during the second heating cycle, there is one clear broad exothermic peak $(T_c = 150°\,C)$ and one endothermic peak $(T_m = 194°\,C)$. On run d during the second cooling, there are two clear resolved crystallization peaks, the first one is broad at $T_{c_1} = 177°\,C$ and the second at $T_{c_2} = 168°\,C$. These results indicate that the material at the start of Run a is the same as at the start of Run c. But from the size of the peaks, it seems that at Run d the material is completely crystallized. It also seems that the original composition is decomposed to, at least, two new compositions.

2. For composition $Se_{0.7}Tl_{0.3}$ (Fig. 3b) the DTA traces of this material show two resolved crystallization peaks $(T_{c_1} = 74°\,C, T_{c_2} = 96°\,C)$ and one melting peak $(T_m = 198°\,C)$. On Run a, from the results, the material is nearly behaving similar to the material of $x = 0.1$ during heating and cooling. However, it seems that the original composition is partially crystalline.

3. For compositions $Se_{0.6}Tl_{0.4}$ (Fig. 3c), the results of the DTA traces show similar behaviour to that of

TABLE II Transition temperatures during two consecutive heating–cooling DTA cycles. The respective rates of heating and cooling were 20 and $15°\,C\,min^{-1}$

Composition	First heating				First cooling				Second heating				Second cooling		
	T_{c_1}	T_{c_2}	T_{m_1}	T_{m_2}	T_{c_1}	T_{c_2}	T_{c_3}	T_{c_4}	T_{c_1}	T_{m_1}	T_{m_2}	T_{m_3}	T_{c_1}	T_{c_2}	T_{c_3}
$Se_{0.9}Tl_{0.1}$	72	102	195	220	134	130			150	194			177	168	
$Se_{0.7}Tl_{0.3}$	74	96	198		187	175			145	197			173		
$Se_{0.6}Tl_{0.4}$	73	120	199		284	175			155	198			284	175	
$Se_{0.5}Tl_{0.5}$			331	367	360				140	201	360		328	267	
$Se_{0.34}Tl_{0.66}$			380		396	385	335		150	383			398	384	334
$Se_{0.3}Tl_{0.7}$			364	375	358	345			371				360		
$Se_{0.2}Tl_{0.8}$			380	395	392	384	345	136	150	380	410		380	306	138
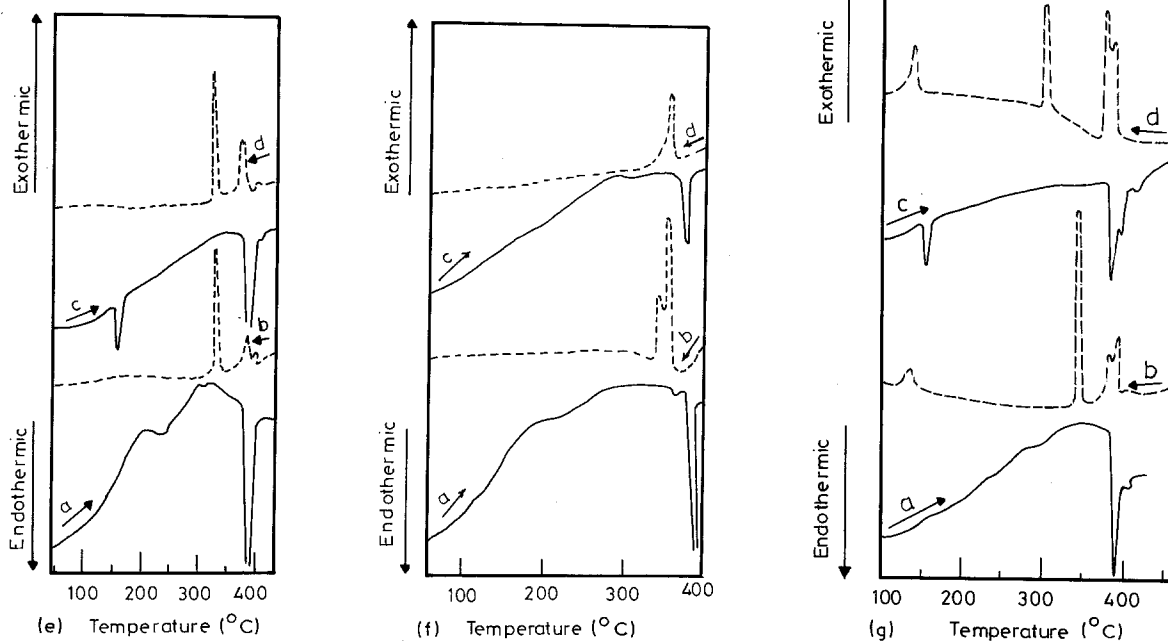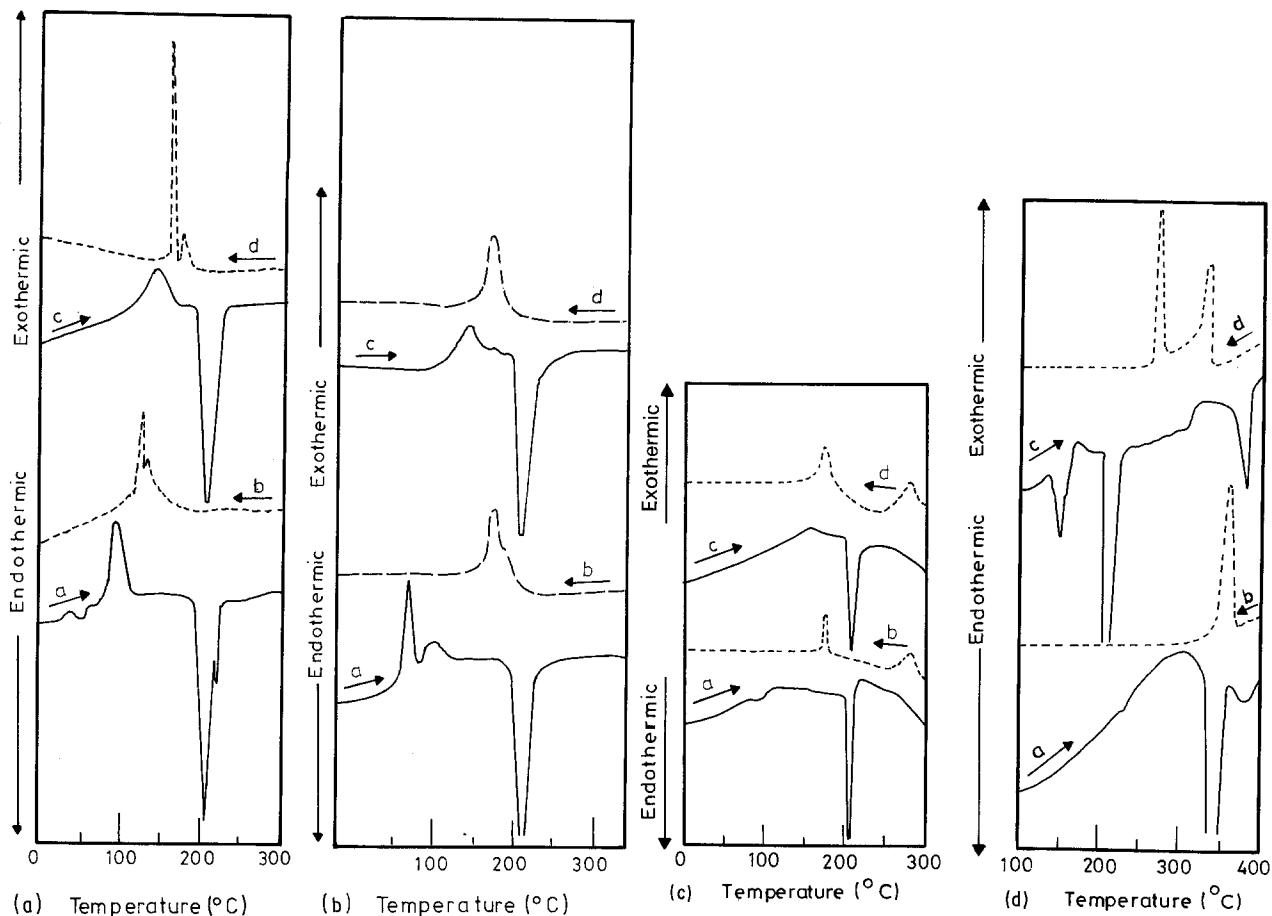
Figure 3 DTA cycling scanning of different compositions of the binary system Tl_xSe_{1-x} : x = (a) 0.1, (b) 0.3, (c) 0.4, (d) 0.5, (e) 0.66, (f) 0.7, and (g) 0.8.

x = 0.3 with some differences (see Table II); e.g. on Run a only two small crystallization peaks appear, and on Runs b and d two small crystallization peaks appear far from each other (T_{c_1} = 284°C, T_{c_2} = 175°C).

4. For composition $Se_{0.5}Tl_{0.5}$ (Fig. 3d), the results of the DTA traces show that at Run a the material is completely crystalline as only two melting peaks appear (T_{m_1} = 331°C large, T_{m_2} = 367°C). One

crystallization peak at T_c = 360°C appears on Run b. Interestingly, on Run c there are three well-resolved melting peaks (T_{m_1} = 140°C, T_{m_2} = 201°C, T_{m_3} = 360°C), and on Run d two well-resolved crystallization peaks (T_{c_1} = 328°C, T_{c_2} = 267°C) appear. Here, it seems that the material at the start of Run a is completely crystalline and at Run c the original composition is decomposed to, at least, three new compositions.

5. For composition $Se_{0.34}Tl_{0.66}$ (Fig. 3e), the results of DTA traces show that at Run a there are traces of crystallization peaks and one large sharp melting peak ($T_m = 380°C$), three crystallization peaks ($T_{c_1} = 396°C$, $T_{c_2} = 385°C$, $T_{c_3} = 335°C$) on Run b, two well-resolved melting peaks ($T_{m_1} = 150°C$, $T_{m_2} = 383°C$) on Run c, and three crystallization peaks on Run d similar in position to the peaks on Run b.

6. For composition $Se_{0.3}Tl_{0.7}$ (Fig. 3f) the DTA indicates on Run a there are two melting peaks ($T_{m_1} = 364°C$, $T_{m_2} = 375°C$), on Run b two unresolved crystallization peaks ($T_{c_1} = 358°C$, $T_{c_2} = 345°C$), on Run c one melting peak ($T_m = 371°C$) and on Run d one broad crystallization peak ($T_c = 360°C$).

7. For composition $Se_{0.2}Tl_{0.8}$ (Fig. 3g), the results of the DTA traces show two melting peaks on Run a ($T_{m_1} = 395°C$, $T_{m_2} = 380°C$) with traces of more melting peaks. On Run b two unresolved crystallization peaks ($T_{c_1} = 392°C$, $T_{c_2} = 384°C$) and another two well-resolved crystallization peaks ($T_{c_3} = 345°C$, large, and $T_{c_4} = 136°C$), appear. On Run c three melting peaks appear ($T_{m_1} = 150°C$, $T_{m_2} = 380°C$, $T_{m_3} = 410°C$). On Run d three well-resolved crystallization peaks appear ($T_{c_1} = 380°C$, $T_{c_2} = 306°C$, $T_{c_3} = 138°C$).

From the results on crystallization behaviour of the system Tl_xSe_{1-x}, with $x = 0.1$ to 0.8, during cycling, one can draw the following conclusions.

1. Only one composition $Se_{0.9}Tl_{0.1}$ shows a glass transition temperature.

2. All compositions used for the cycling experiments are partially or completely crystalline at the start.

3. Increasing the thallium content decreases the probability of obtaining a glassy composition and this is clear from the DTA traces, e.g. compositions with $x = 0.1, 0.3$, and 0.4 showed crystallization peaks and the size of the crystallization peaks decreases with increasing thallium content.

4. The crystallization peak on Run c begins at a higher temperature than that on Run a, indicating that the crystallization is easier in the powdered material.

5. The system Tl_xSe_{1-x} is unstable and it can be decomposed by heat cycling.

6. It may be possible to obtain one stable composition near $x = 0.7$.

7. From Run a for all compositions, it seems that T_m increases with thallium content.

6. Crystallization kinetics

Prior studies made by Kotkata et al. [6–9] on various glassy systems have shown the utility of a simple DTA model using a single-scan technique for studying thermally activated crystallization phenomena in amorphous chalcogenide semiconductors. In this model, the transformed fraction (α) is proportional to the relevant area under the DTA exothermic peak. The conditional requirements of the model have been given in [6], and its consequences are reviewed below.

To obtain convenient DTA curves for kinetic analysis, a slow constant scan rate $\phi = dT/dt$ of $2°C\,min^{-1}$ and a relatively high speed of the recorder chart have

been considered. The variation of α with the heating temperature for Se and Tl–Se glasses are shown in Fig. 4 for both first and second exothermic peaks. The curves are sigmoidal in shape indicating an autocatalytic reaction as is often observed in various kinds of solid reactions.

An estimation of the complex activation energy of crystallization (E) can be made by using Piloyan et al.'s method [10]. This is based on the differential form of the model relation for α, known as $g(\alpha)$, and on Borchard's assumption [11] that the reaction rate, $d\alpha/dt$, is proportional to the temperature deflection, ΔT, as detected by DTA. This means that the kinetic equation

$$-\ln (1 - \alpha) = K_0 t^n \exp (-E/RT) \qquad (1)$$

which was formally derived by Avrami [12–14], has been differentiated to yield

$$d\alpha/dt = nK_0^{1/n} \exp (-E/RT)^{1/n} f(\alpha) \qquad (2)$$

where

$$f(\alpha) = (1 - \alpha) [-\ln (1 - \alpha]^{(n-1)/n}$$

Here, K_0 is considered to be constant with respect to temperature. For a constant heating rate $\phi = dT/dt$, Equation 2 is separable in α and T and can therefore be directly integrated

$$\int_0^\alpha \frac{d\alpha}{(1 - \alpha)[\ln (1 - \alpha)^{-1}]^{(n-1)/n}}$$

$$= \frac{nK_0^{1/n}}{\phi} \int_0^T \exp \frac{(-E)}{nRT} dT \qquad (3)$$

Integration yields,

$$[\ln (1 - \alpha)^{-1}]^{1/n} = \frac{EK_0^{1/n}}{\phi R} P(x) = g(\alpha) \qquad (4)$$

where $x = E/nRT$ and the behaviour of the exponential integral function $p(x)$ when different types of approximations are used has been reviewed in [15]. For a limited range formula, i.e. normal temperature interval of about $100°C$, $p(x) = \exp (x)$. Therefore, Equation 3 can be written in a logarithmic form as

$$\log [g(\alpha)] = C - \frac{E}{2.303\,nRT} \qquad (5)$$

where C is a constant.

Calculation of the function $g(\alpha)$ has been carried out by Satava and Skavara [16] for different reaction kinetic equations. A plot of $\log [g(\alpha)]$ against $1/T$ should give a straight line over the whole range of $\alpha(0 < \alpha < 1)$ when the appropriate mathematical description of the reaction is employed. From the slope of the straight line, the value of E/n can be obtained. Typical plots of $\log [g(\alpha)]$ against $1/T$ are given in Fig. 5 for the first peaks of three different compositions (as examples) for the different rate-controlling processes with the functions labelled according to the symbols given by Sharp et al. [17]. This figure shows that the function $A_3(\alpha)$ where $-\ln (1 - \alpha)^{1/3} = Kt$, is in agreement with the experimental calculations over a maximum range of α. A least squares fit for the experimental points indicates that deviations from linearity are comparatively very
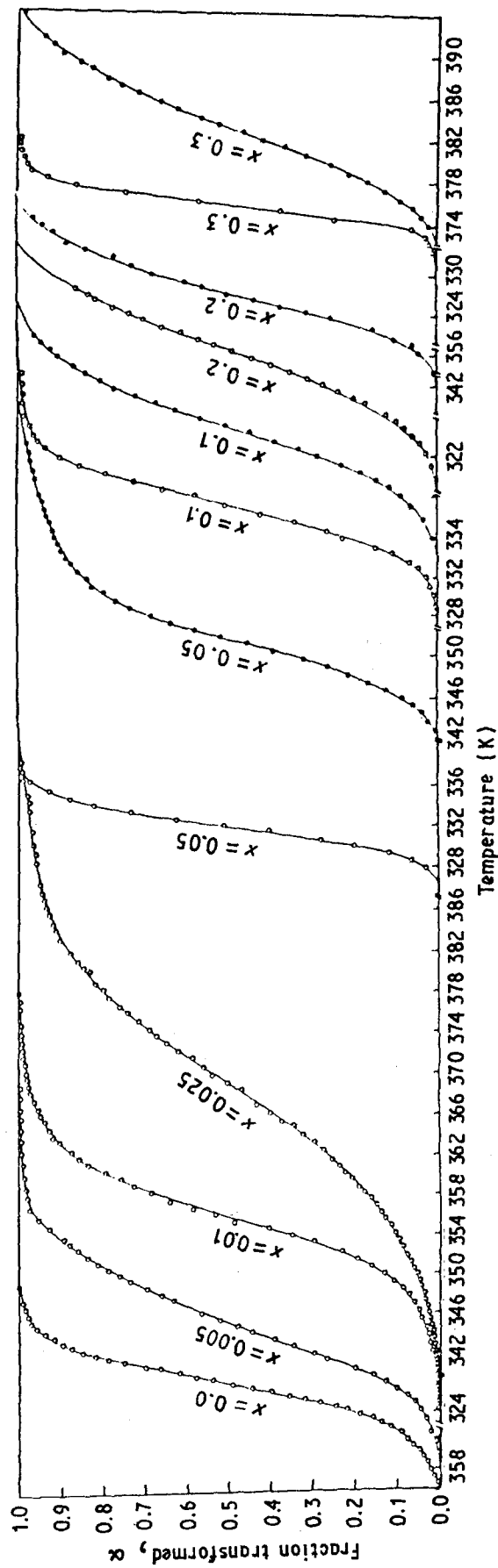
Figure 4 The temperature dependence of the integrated transformed fraction (α) as calculated from the area under DTA first (O) and second ($\bullet$) exothermic peaks of Tl_xSe_{1-x} glasses.
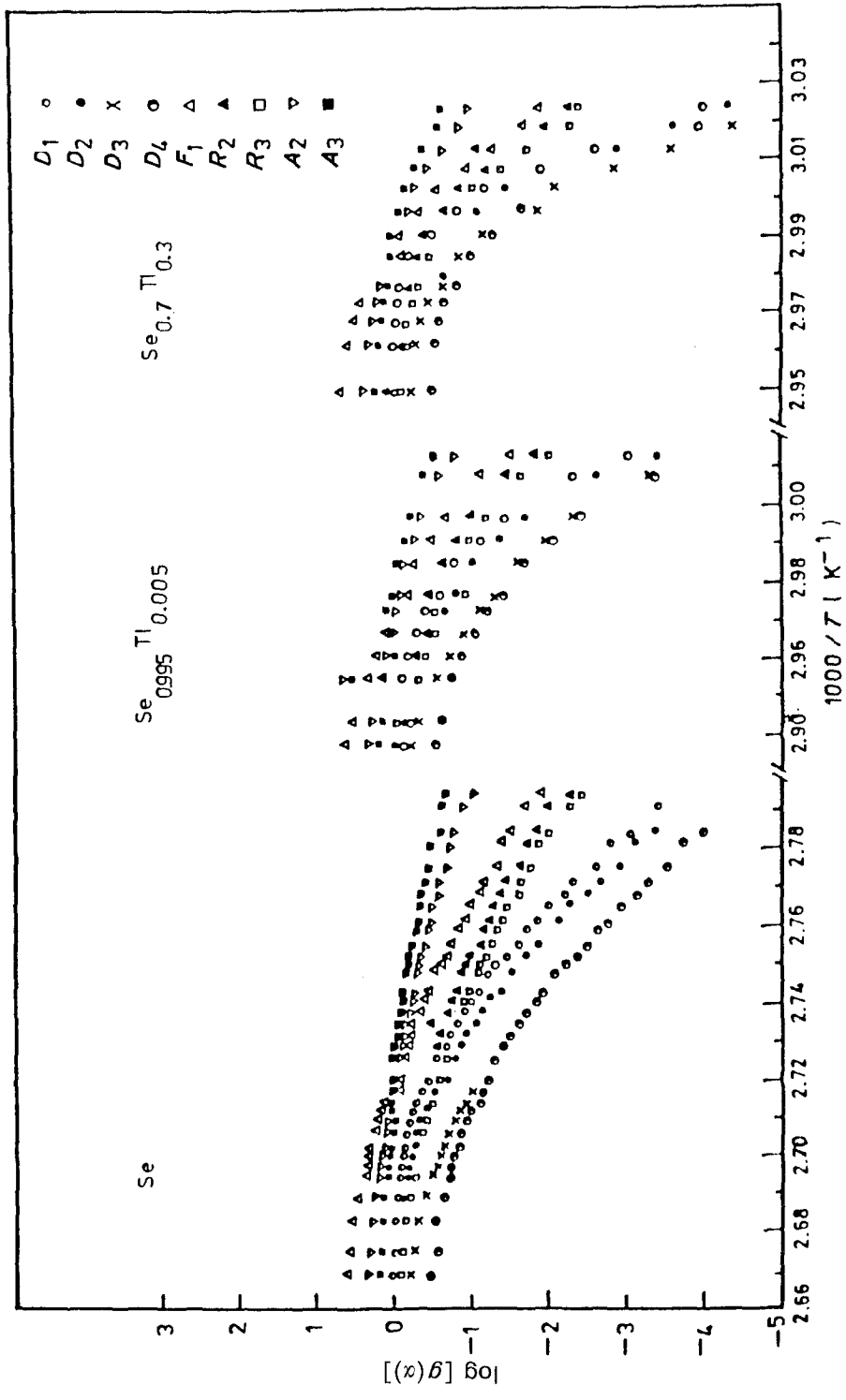
Figure 5 Plots of log [g(α)] against 1/T for the crystallization of some Tl_xSe_{1-x} samples calculated for various kinetic equations. The functions are labelled according to the symbols g
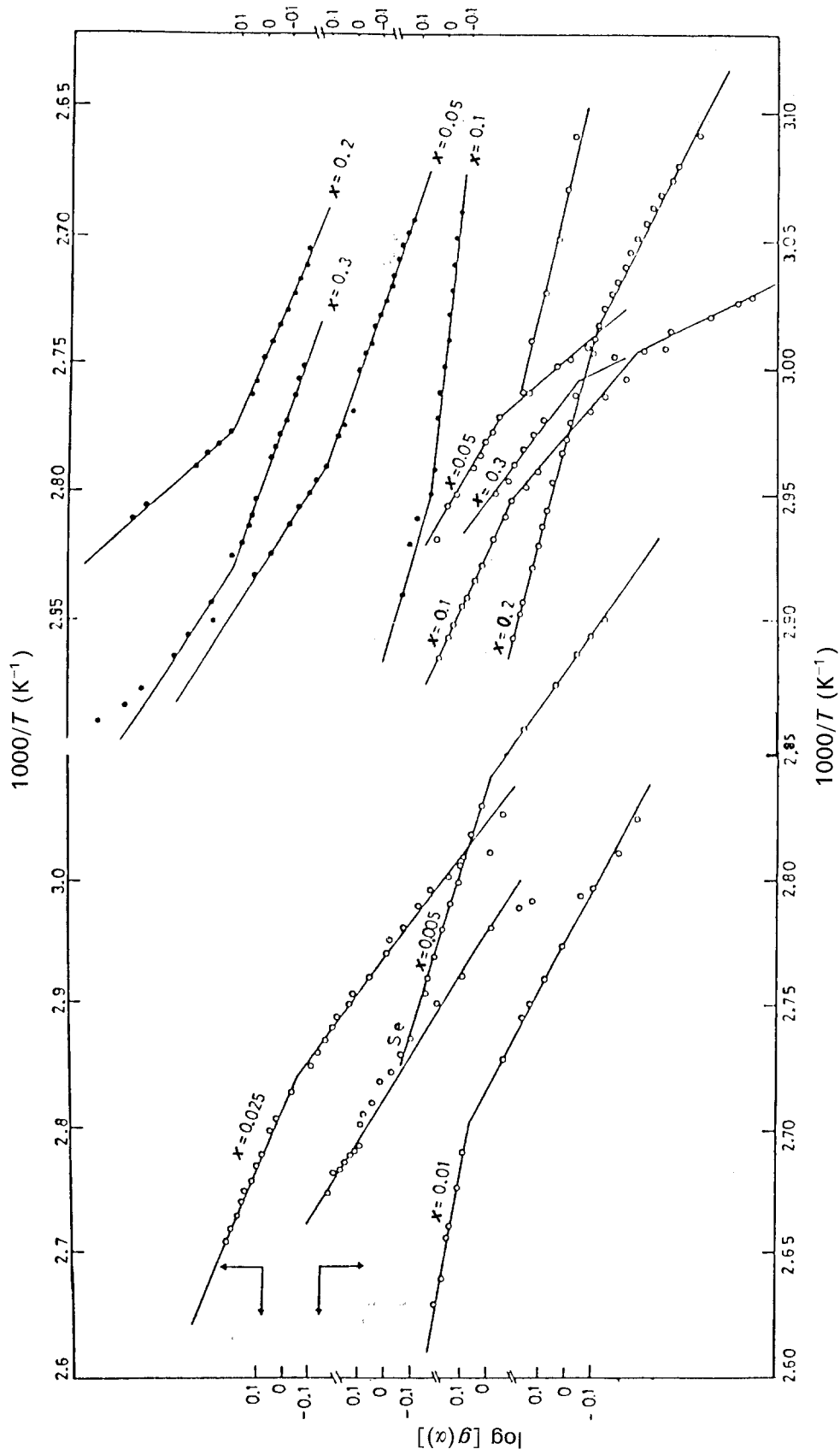
Figure 6 Plots of log |g(α)| against 1/T for the most probable reaction kinetic function of each glassy composition of the system Tl$_x$Se$_{1-x}$:(O) first peak, (●) second peak.
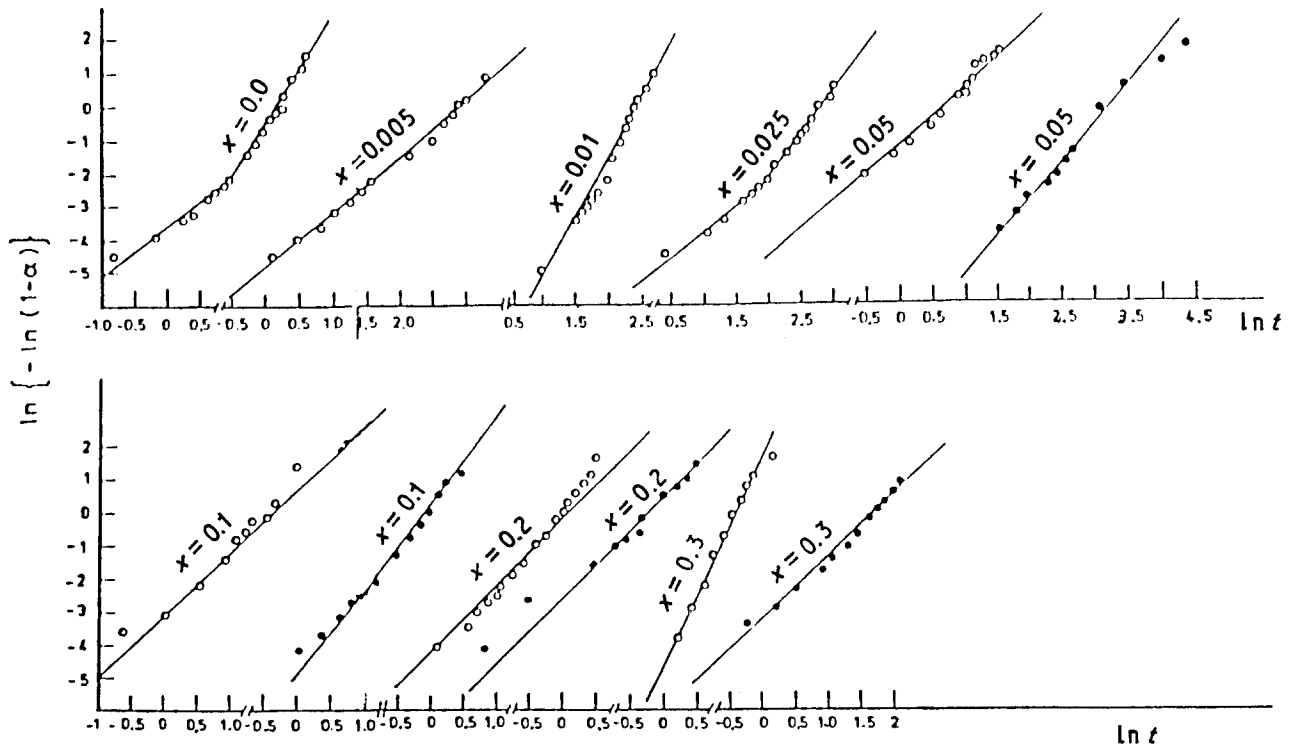
Figure 7 Avrami's plots, ln [−ln (1−α)] against ln (*t*), for the investigated glasses of the system Tl_xSe_{1-x} :(O) first peak, (●) second peak.

small for the function $A_3(\alpha)$, where the fitting region of α is almost 0.01 to 0.99.

In Fig. 6, log [$g(\alpha)$] is plotted against $1/T$ for the Tl–Se alloy studied. In this figure, only the most probable reaction mechanism for the devitrification process of each composition is presented. The function $A_3(\alpha)$ was found to approximate linear behaviour closely over the entire range of α for all the compositions except the composition of $Se_{0.975}Tl_{0.025}$ where the function $A_2(\alpha)$ (i.e. $-\ln (1-\alpha)^{1/2} = Kt$) gives better fitting. For some compositions, fitting of log [$g(\alpha)$] curves can be achieved through two distinct slopes. This indicates that the crystallization process proceeds through two different rates.

According to Avrami's equation [12]

$$\alpha = 1 - \exp (-Kt^n) \qquad (6)$$

which can be written in a logarithmic form as

$$\ln [-\ln (1 - \alpha)] = \ln K + n \ln t \qquad (7)$$

A plot of ln [−ln (1 − α)] against ln *t* should yield a straight line whose slope is *n* and intercept on the ordinate at ln *K*. The value of *n*, which reflects the

nucleation rate and the growth morphology, is correlated with the effective activation energy, (E/n), obtained from the slope of log [$g(\alpha)$] against $1/T$, to estimate the activation energy of crystallization (E).

The fitting of Avrami's equation has been carried out using the computer facilities to check the reliability and limitation of the lines. Fig. 7 shows the relation between ln [−ln (1 − α)] and ln *t* for the Tl–Se compositions investigated. The values of *n*, *K* and *E* are evaluated and are given in Table III. Here, it is worth noting that only the average values of *E* and *n* are given in the table for the compositions in which the relations log [$g(\alpha)$]–$1/T$ and/or ln [−ln (1 − α)]–ln *t* are represented by two distinct slopes.

Table III indicates that the values of *n* lie in the range 1.5 and 4.3 for the low-temperature phase and in the range of 1.8 to 2.6 for the high-temperature phase. These correspond to a non-monotonic relative variation for the reaction rate *K* as 2.7 × 10⁻⁴ to 5.5 × 10⁻² and 1.2 × 10⁻² to 7.4 × 10⁻². In addition, the relative corresponding variation for *E* is 1.0 to 4.5 eV and 1.7 to 2.5 eV. The corresponding controlling mechanism [$A_2(\alpha)$ or $A_3(\alpha)$] is written along side each composition.

TABLE III Crystallization kinetic parameters of Tl_xSe_{1-x} glasses as a function of thallium content alongside the most probable reaction function

Composition	−ln *K*		*n*		*E*(eV)		Function
	Low-temp. phase	High-temp. phase	Low-temp. phase	High-temp. phase	Low-temp. phase	High-temp. phase	
Se	4.5		1.5		1.8		A_3
$Se_{0.995}Tl_{0.005}$	4.3		2.0		2.8		A_3
$Se_{0.99}Tl_{0.01}$	8.2		3.2		2.2		A_3
$Se_{0.975}Tl_{0.025}$	6.4		2.1		1.0		A_2
$Se_{0.95}Tl_{0.05}$	3.0	4.0	3.0	2.2	3.4	2.5	A_3
$Se_{0.9}Tl_{0.1}$	2.9	4.4	1.8	2.6	1.7	1.9	A_3
$Se_{0.8}Tl_{0.2}$	4.2	2.6	2.0	1.9	1.6	1.7	A_3
$Se_{0.7}Tl_{0.3}$	4.4	3.20	4.3	1.8	4.5	2.3	A_3

References

1. H. E. KISSINGER, *J. Res. Nat. Bur. Stand.* **57** (1956) 217.
2. H. E. KISSINGER, *Analyt. Chem.* **29** (1957) 1702.
3. M. F. KOTKATA *et al.*, *Acta Phys. Hung.* **68** (1990) in press.
4. M. F. KOTKATA *et al.*, *J. Non-Cryst. Solids* **97, 98** (1987) 1259.
5. D. TURNBULL, *J. Phys. Chem.* **66** (1962) 609.
6. M. F. KOTKATA and E. A. MAHMOUD, *Mater. Sci. Eng.* **54** (1982) 163.
7. M. F. KOTKATA *et al.*, *ibid.* **60** (1983) 163.
8. M. F. KOTKATA, M. H. EL-FOULY and M. B. EL-DIN, *Latin. Amer. J. Metall. Mater.* **5** (1985) 28.
9. M. F. KOTKATA and C. S. MOHAMED, *J. Mater. Sci.* **24** (1989) 1291.
10. F. O. PILOYAN, I. O. RYABCHIKOV and O. S. NOVIKOVA, *Nature* **212** (1966) 1229.
11. H. J. BORCHARD, *J. Inorg. Nucl. Chem.* **12** (1960) 252.
12. M. AVRAMI, *J. Chem. Phys.* **7** (1939) 1103.
13. *Idem ibid.* **8** (1940) 212.
14. *Idem ibid.* **9** (1941) 177.
15. J. SESTAK, *Thermochim. Acta.* **3** (1971) 150.
16. V. SATAVA and F. SKAVARA, *J. Amer. Ceram. Soc.* **52** (1969) 591.
17. J. H. SHARP, G. V. BRINDLEY and B. N. N. ACHAR, *ibid.* **49** (1966) 379.